

22. SOME RECENT STUDIES OF HIGH-LIFT FLAPS

ON COMPOSITE WING PLANFORMS

By Alexander D. Hammond
NASA Langley Research Center

22

SUMMARY

Over the years techniques for generating very high lift have been developed by NACA, NASA, and other research establishments. Work on mechanical flap systems to achieve high lift resulted in the development of the double-slotted flap which, in a full-span configuration, is capable of achieving lift coefficients up to 3 and 4.

The purpose of this paper is to present the results of some recent investigations which show the application of the previously developed double-slotted-flap systems to attain high lift on the newer composite wing planforms such as the variable-sweep wing.

The application of double-slotted-flap systems to composite wing planforms results in configurations capable of efficiently developing high lift if careful attention is paid to the details of the design of the system. It is shown herein that leading-edge slats are an essential part of the high-lift system. A moderate sized wing glove was found to have negligible effect on the lift and drag of an efficient high-lift system but was detrimental insofar as the longitudinal stability is concerned.

Adequate determination of flow separation effects on wings with high-lift devices, especially near maximum lift, requires that tests be made at Reynolds numbers as high as possible. The necessity for testing over a moving-belt ground board to determine the ground effects depends on the lift developed by the high-lift system and the height of the lifting system above the ground plane.

INTRODUCTION

Over the years techniques for generating very high lift have been developed and demonstrated by NACA, NASA, and other research establishments. Work on mechanical flap systems to achieve high lift resulted in the development of the single-slotted and double-slotted flaps capable of achieving lift coefficients up to 3 and 4. (See refs. 1 to 8.) The purpose of this paper is to present the results of some recent investigations which show the application of the previously developed double-slotted-flap systems to attain high lift on the newer composite wing planforms such as the variable-sweep wing.

Preceding page blank

SYMBOLS

C_L	lift coefficient, $\frac{\text{Lift}}{qS}$
C_D	drag coefficient, $\frac{\text{Drag}}{qS}$
C_m	pitching-moment coefficient, $\frac{\text{Pitching moment}}{qS\bar{c}}$
$C_{m, \bar{c}/4}$	pitching-moment coefficient referred to quarter-chord point of wing mean aerodynamic chord, $\frac{\text{Pitching moment}}{qS\bar{c}}$
A	wing aspect ratio, b^2/S
b	wing span, inches
c	wing chord, inches
\bar{c}	wing mean aerodynamic chord, inches
h	height of wing chord plane above the ground, inches
i_t	tail incidence angle, degrees
Δp	increment in static pressure between wing upper surface and wing lower surface, pounds/foot ²
q	free-stream dynamic pressure, pounds/foot ²
R	free-stream Reynolds number per foot
S	wing area, feet ²
x	chordwise distance from wing leading edge, inches
α	wing angle of attack, degrees
δ_f	flap deflection, degrees
δ_{slat}	slat deflection, degrees
Λ	leading-edge sweep angle, degrees
$\Lambda_{c/4}$	sweep of wing quarter-chord line, degrees

DISCUSSION

Review of Fundamentals

Figure 1 shows sketches of a double-slotted flap in the retracted and deflected positions. A large-chord flap, a vane, and a leading-edge slat can be stored within the contour of a relatively thin airfoil as indicated by the cross section drawing for a typical wing station. When the high-lift system is deflected as shown in the lower sketch, it is desirable to have a smooth upper-surface contour with the camber distributed over the entire wing chord insofar as possible. For this reason, it is desirable to have a large-chord flap, from 30 to 40 percent of the wing chord, and a vane with a chord of about half the flap chord, so that the flap can be extended as far as possible. This chord extension increases the wing area and also provides for a smooth camber line. Flow through the slots provides some boundary-layer control on the flap and vane. It is important for the slots to be convergent, that is, for the minimum area to occur at the slot exit. Although the flap illustrated is a double-slotted flap, the rear flap can be divided into two parts with another slot between them to form a triple-slotted flap to attain higher usable flap deflections.

The leading-edge slat has a chord of about 15 percent of the wing chord and there is a gap between the slat and the wing leading edge to provide boundary-layer control. Most high-lift systems need leading-edge devices as is illustrated by the chordwise load distributions shown in figure 2. The plot on the left of figure 2 illustrates the typical chordwise load distribution as the result of angle of attack with the peak load at the leading edge of the airfoil. When the double-slotted flap is deflected to 35° , the flap load distribution is added to the angle-of-attack distribution. High pressure peaks occur at the flap and vane leading edges and the peak at the wing leading edge would also be increased. However, because of the increase in the adverse pressure gradient that would accompany this increase in the leading-edge peak pressure, separation often occurs, and the increase in leading-edge pressure is not realized. When a slat is deflected in front of the wing, the leading-edge separation is alleviated and the lift peak on the front part of the airfoil is restored. Higher lift is obtained as a result of the alleviation of the separation effects and the chord extension provided by the slat.

Composite Wing Configurations

Sketches of the composite wing configurations used in a recent high-lift investigation at the Langley Research Center are shown in figure 3. The tests were made in the 17-foot test section of the Langley 300-MPH 7- by 10-foot tunnel. The basic wing configuration shown here had an unswept wing with a span of 120 inches and an aspect ratio of 10; it was equipped with a double-slotted-flap high-lift system shown in figure 3. The double-slotted flap was full span and extended from wing tip to wing tip even underneath the fuselage. The configuration was tested with and without the 70° swept-wing glove shown by the shaded area. When the glove was in place, the leading-edge slat extended from

the intersection of the wing and glove to the wing tips. Without the glove, the slat extended from the fuselage to the wing tip. The high-lift devices with and without the wing glove were also tested at wing sweeps of 15° and 25° . Although the wing span was greater for the swept wings, the aspect ratio of all three wings was approximately the same. The coefficients for each wing configuration are based on the geometry of each wing without the wing glove.

The effect of the leading-edge slat on the 15° swept-wing configuration is shown in figure 4. The maximum lift for the wings with the leading-edge slat on is higher for both flap deflections. It can also be seen that the onset of separation for the 40° flap deflection, indicated by a decrease in lift-curve slope at an angle of attack of about 1° , is delayed to a higher angle of attack with the leading-edge slat on.

The data for the basic wing without the high-lift devices were used to compute the envelope drag polar shown by the dashed curve in figure 4. That is, the basic wing-span efficiency factor of 0.89 and the zero-lift drag of a symmetrical airfoil of the same thickness were used to compute the curve. It can be seen that the full-span high-lift system has about the same span efficiency as the basic wing, since the drag data for the high-lift devices are tangent to the envelope drag curve at high lift coefficients.

The effect of wing sweep for the wings with 40° flap deflection and leading-edge slats is shown in figure 5. As the wing sweep is increased, the lift decreases and the induced drag becomes larger. However, it should be pointed out that the flap span on the 25° swept wing extended only from the wing-fuselage junction to the wing tip and that part of the lift loss shown results from the flap span effects. In fact, if the loss of lift resulting from sweep is calculated by the method of reference 9, the lift at zero angle of attack for the 25° swept wing would fall at the tick mark. The calculated loss of lift due to the reduction in flap span then reduces the lift further so that the increment between the unswept wing and the 25° swept wing at zero angle of attack agrees with the total computed loss. The lift loss shown for the 15° swept wing is almost all due to wing sweep since this wing has nearly a full-span flap.

The data shown in figure 6 indicate that there is very little, if any, effect of the wing glove on either the lift or drag for any of the wing sweeps and further indicate that, for a glove this size, a composite wing can develop the same lift as the basic wing without the glove. However, the distribution of this lift will change as indicated by the pitching-moment data shown in figure 7. The pitching-moment coefficients for the same flap configuration are shown for the 0° , 15° , and 25° swept wings. There is a forward shift of the lift load with the leading-edge glove on as indicated by the change in slope of the pitching-moment curves between the glove-off and glove-on curves. However, there is very little change in the variation of the pitching moment with angle of attack for a glove this size.

The results of some tests reported in reference 10 on a variable-sweep model for which the sweep of the glove leading edge was varied from 60.4° to 70° and then to 75° are shown in figure 8. The glove area increased as the glove sweep increased. The wing was equipped with a double-slotted flap deflected to 50° in combination with a leading-edge slat that extended across

the outer wing panel. Again there is very little effect of the glove on the lift and drag characteristics. There is, however, a definite destabilizing effect of the glove on the pitching-moment characteristics. The previous pitching-moment data (fig. 7) were for a tail-off configuration and these data are for a tail-on configuration. However, the data for this model with the tail off show the same destabilizing pitching-moment trends as are shown for the tail-on configuration, although the trends were not as pronounced - an indication that there are some changes in the flow at the tail as a result of the glove. This destabilizing effect of the wing glove with the high-lift configuration has also been shown for the unflapped wing at low lift coefficients by Ray, Lockwood, and Henderson in paper no. 5.

Reynolds Number Effects

In any discussion of the results of high-lift investigations, the effects of Reynolds number must always be considered. Shown in figure 9 are some results from an investigation of a model of a current fighter in the Ames 12-foot pressure tunnel at the Reynolds numbers shown. The data are for a complete model with a slat deflection of 45° , a flap deflection of 40° , and for a tail incidence of -10° . The data for a Reynolds number of 1.89×10^6 indicate a very low maximum lift as well as premature separation as shown by the high drag and the early breaks in the slopes of the lift-coefficient and pitching-moment curves. The data for a Reynolds number of 3.21×10^6 do not attain a maximum lift as high as the data for 5.97×10^6 , but do, however, show the same initial lift-curve and pitching-moment breaks. These results emphasize that tests should be made at Reynolds numbers high enough to determine the flow separation effects adequately, especially near maximum lift.

Ground Simulation

One other subject relating to testing techniques involved with high-lift investigations is the proper ground simulation to determine the ground effects. The significance of the ground effect has been discussed in paper no. 19 by Kemp, Lockwood, and Phillips and in paper no. 20 by Rolls, Snyder, and Schweikhard. The use of the moving-belt ground board for determining ground effects is presented in reference 11, and results for configurations with double-slotted flaps are summarized in figures 10 and 11.

Figure 10 shows the effect of ground simulation on the lift, drag, and pitching-moment characteristics of the double-slotted flaps on the unswept-wing configuration discussed previously. The out-of-ground-effect data are compared with data taken at $h/b = 0.06$ above a fixed ground plane and at the same height over a moving ground plane. The point here is not to show the ground effects as such but to show that, up to a lift coefficient of about 1.6, both methods of ground simulation give the same results. However, at lift coefficients above 1.6, at this ground height, the fixed-ground-board method of ground simulation shows too large an effect of ground. These data indicate that, at this height, tests can be made on configurations developing lift coefficients up to 1.6 without the need for a moving ground plane. Other data for this lifting system at different heights indicate the same general trend. A

correlation of lift coefficient and ground height was made in reference 11 for this configuration and other full-span flap systems (with aspect ratios from 6 to 10), to show when it is necessary to have a moving ground plane. The conditions requiring moving ground board for proper ground simulation are shown in figure 11. The symbols represent data points used to establish the boundary shown. For lift coefficients attained at ground heights that fall above the boundary, a conventional ground board is adequate. If the lift coefficient attained for a given ground height falls below the boundary, a moving ground plane would be needed to determine the effects of the ground properly. The lift coefficients developed by low-aspect-ratio wings at the minimum heights allowed for by the landing gear generally fall in the area above the boundary where a conventional fixed ground board would provide adequate ground simulation.

CONCLUDING REMARKS

The application of previously developed mechanical high-lift systems to composite wing planforms resulted in configurations capable of efficiently developing high lift, if careful attention is paid to details of the design of the system. It has been shown that leading-edge slats are an essential part of the high-lift system.

The effect of a moderate sized wing glove was found to be negligible on the lift and drag of an efficient high-lift system but is detrimental insofar as the longitudinal stability is concerned.

Tests of high-lift devices should be made at Reynolds numbers as high as possible in order to determine adequately the effects of flow separation on the high lift characteristics, especially near maximum lift.

The necessity for testing over a moving ground board to determine the ground effects depends on the lift developed by the high-lift system and the height of the lifting system above the ground plane.

REFERENCES

1. Abbott, Ira H.; and Von Doenhoff, Albert E.: Theory of Wing Sections. Dover Publ., Inc., 1959.
2. Cahill, Jones F.: Summary of Section Data on Trailing-Edge High-Lift Devices. NACA Rept. 938, 1949. (Supersedes NACA RM L8D09.)
3. Young, A. D.: The Aerodynamic Characteristics of Flaps. R. & M. No. 2622, British A.R.C., Feb. 1947.
4. Riebe, John M.: A Correlation of Two-Dimensional Data on Lift Coefficient Available With Blowing-, Suction-, Slotted-, and Plain-Flap High-Lift Devices. NACA RM L55D29a, 1955.
5. Schwartzberg, Milton A.; and Burch, John L.: Lifting Capabilities of Wings With and Without High-Lift Devices. Eng. Rept. No. 8055 (Contract NOa(s)55 655-c), The Glenn L. Martin Co., Apr. 1956.
6. Dike, D. J.; Dunn, H. S.; Hazen, D. C.; and Lehnert, R. F.: A Study of the Low Speed Aerodynamic Characteristics of High-Lift Flow Controlled Profiles and Wings. Rept. No. 349 (Contract No. Noas 55-583-d), Dept. Aeron. Eng., Princeton Univ., May 1958.
7. Naeseth, Rodger L.; and Davenport, Edwin E.: Investigation of Double Slotted Flaps on a Swept-Wing Transport Model. NASA TN D-103, 1959.
8. Henderson, William P.; and Hammond, Alexander D.: Low-Speed Investigation of High-Lift and Lateral Control Devices on a Semispan Variable-Sweep Wing Having an Outboard Pivot Location. NASA TM X-542, 1961.
9. Lowry, John G.; and Polhamus, Edward C.: A Method for Predicting Lift Increments Due to Flap Deflection at Low Angles of Attack in Incompressible Flow. NACA TN 3911, 1957.
10. Lockwood, Vernard E.: High-Lift Characteristics of a Variable-Sweep Supersonic Transport Model With a Blended Engine-Fuselage and Engine-Mounted Horizontal Tails. NASA TM X-1199, 1966.
11. Turner, Thomas R.: Endless-Belt Technique for Ground Simulation. Conference on V/STOL and STOL Aircraft, NASA SP-116, 1966, pp. 435-446.

DOUBLE-SLOTTED FLAP AND SLAT

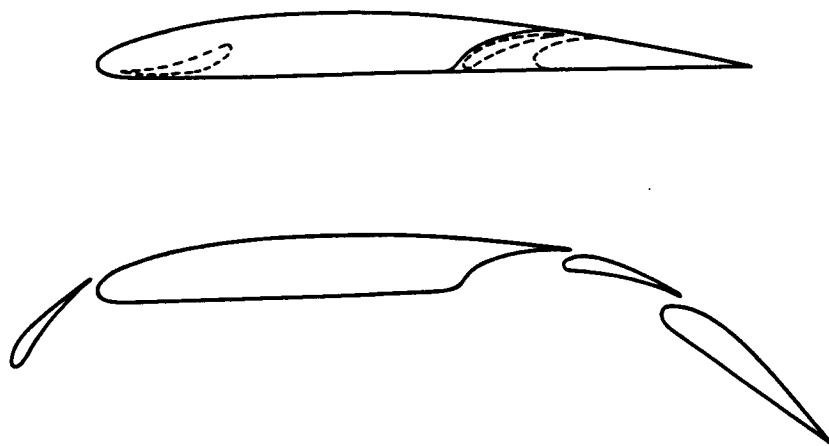


Figure 1

CHORDWISE LOAD DISTRIBUTION

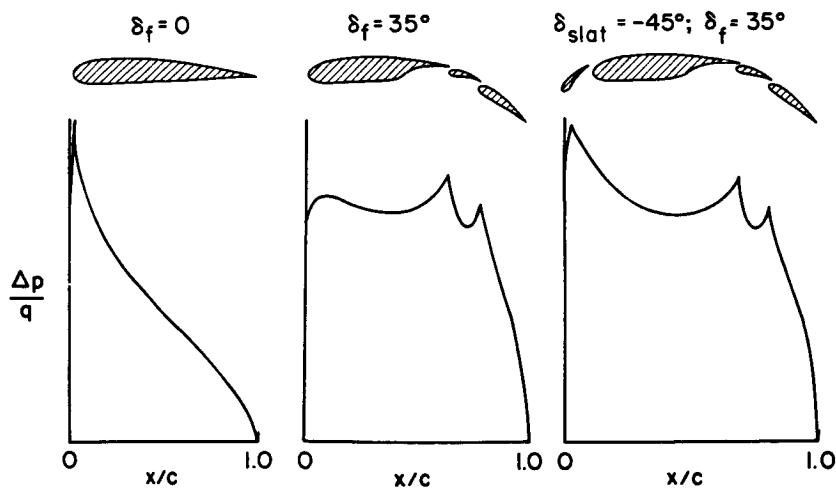


Figure 2

COMPOSITE WING CONFIGURATIONS
HIGH-LIFT INVESTIGATION

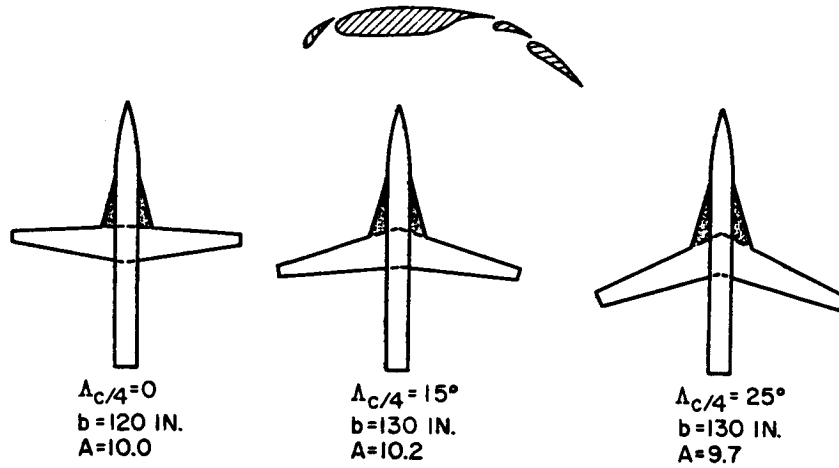


Figure 3

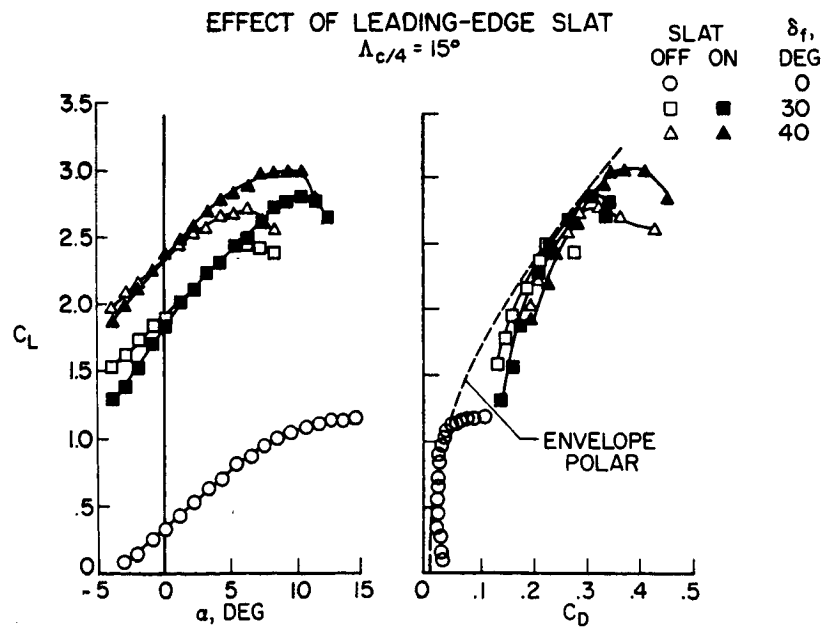


Figure 4

EFFECT OF WING SWEEP
 $\delta_f = 40^\circ$; SLAT ON

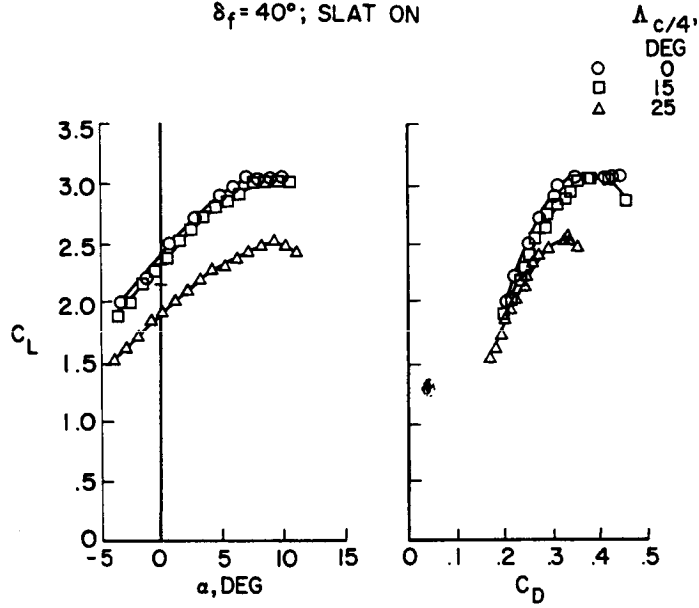


Figure 5

EFFECT OF LEADING-EDGE GLOVE
 $\delta_f = 40^\circ$; SLAT ON

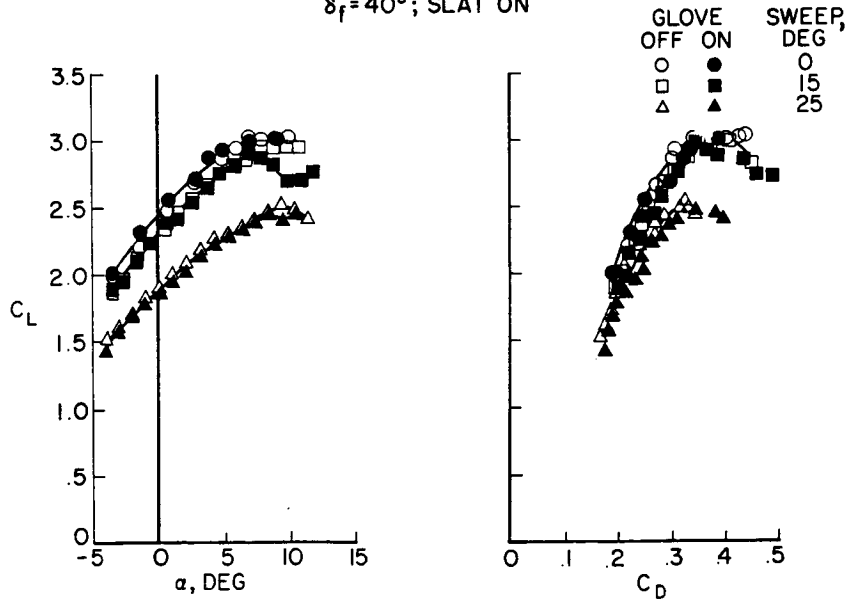


Figure 6

EFFECT OF LEADING-EDGE GLOVE
 $\delta_f = 40^\circ$; SLAT ON

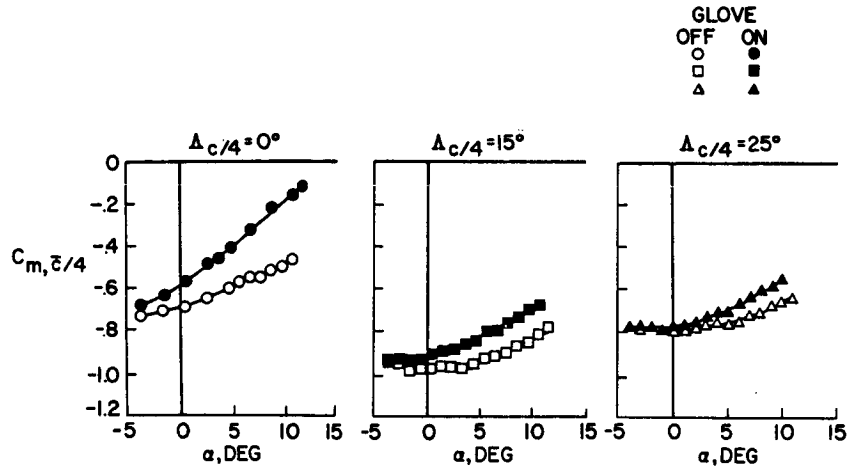


Figure 7

EFFECT OF GLOVE SWEEP
 $\delta_f = 50^\circ$; $i_f = -10^\circ$

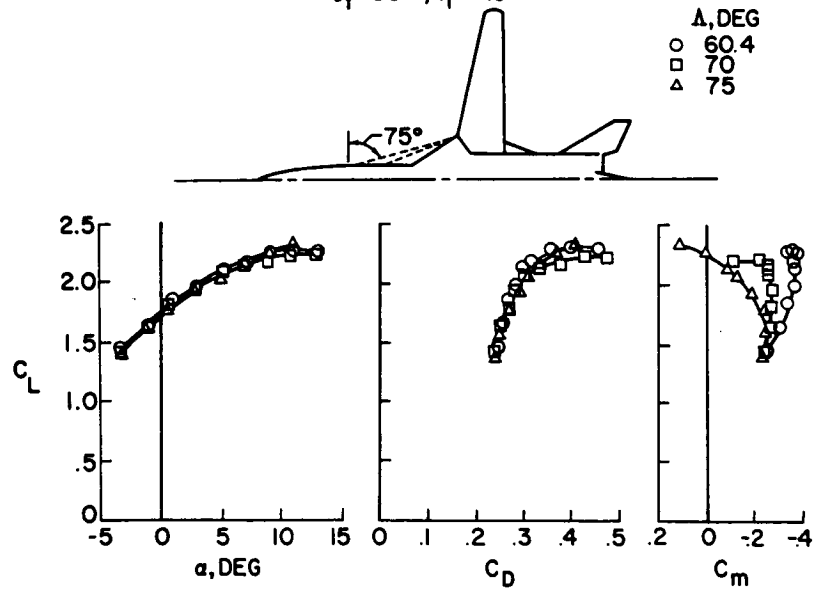


Figure 8

EFFECT OF REYNOLDS NUMBER

$\delta_{slat} = -45^\circ; \delta_f = 40^\circ; i_f = -10^\circ$

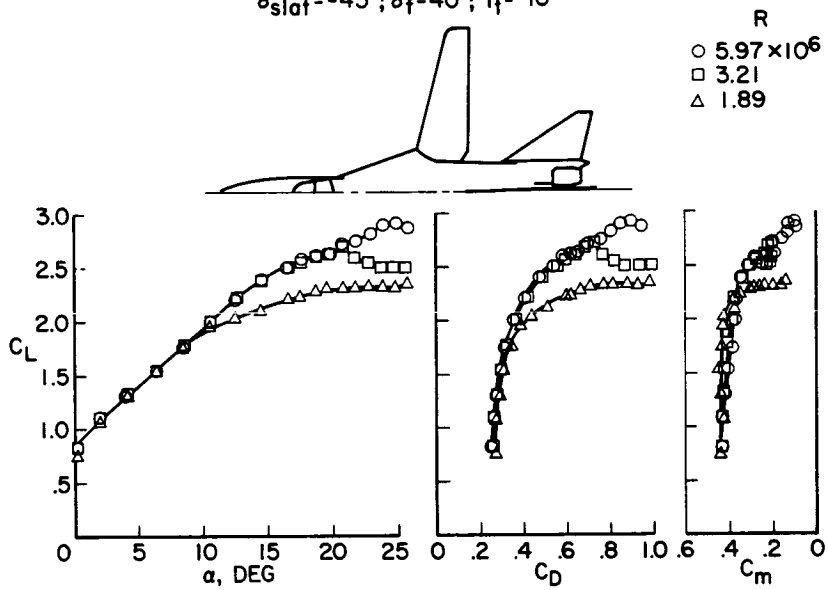


Figure 9

EFFECT OF GROUND SIMULATION

h/b
 \circ ∞
 \square .06 FIXED BOARD
 \triangle .06 MOVING GROUND

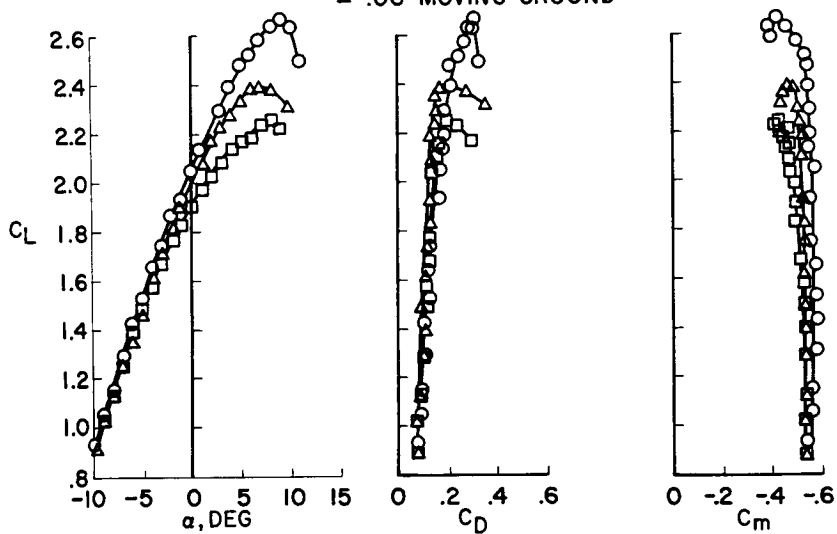


Figure 10

CONDITIONS REQUIRING MOVING GROUND BOARD
FULL-SPAN HIGH-LIFT DEVICES

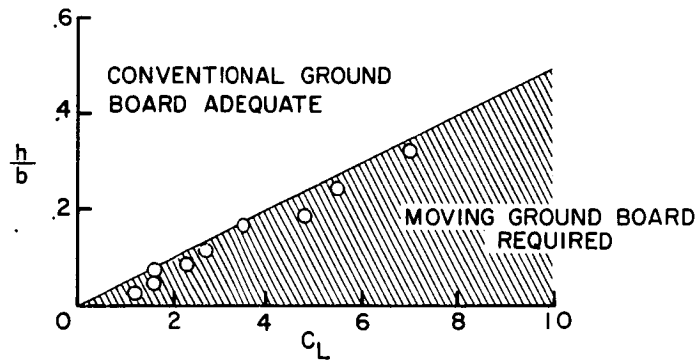


Figure 11